ISSN 1064-2269, Journal of Communications Technology and Electronics, 2015, Vol. 60, No. 9, pp. 952–957. © Pleiades Publishing, Inc., 2015.
Original Russian Text © A.P. Anyutin, I.P. Korshunov, A.D. Shatrov, 2015, published in Radiotekhnika i Elektronika, 2015, Vol. 60, No. 9, pp. 896–901.

ELECTRODYNAMICS AND WAVE PROPAGATION

Plasmon Resonances in a Quartz Nanofiber Coated with a Silver Layer

A. P. Anyutin, I. P. Korshunov, and A. D. Shatrov

Kotel'nikov Institute of Radio Engineering and Electronics, Fryazino Branch, Russian Academy of Sciences, pl. Vvedenskogo 1, Fryazino, Moscow oblast, 141190 Russia

e-mail: anioutine@mail.ru; korip@ms.ire.rssi.ru

Received February 16, 2015

Abstract—A 2D problem of diffraction of the TM-polarized plane wave by a quartz nanofiber coated with a silver layer is investigated. The total scattering cross-section is numerically calculated in the range of visible light waves (400–700 nm). It is found that, at certain geometric parameters of the structure, not only dipole but also multipole plasmon resonances arise in the investigated range of wavelengths. Scattering patterns at resonance frequencies are calculated. It is demonstrated that deposition of the silver layer onto a quartz nanofiber can decrease the scattering cross section several times.

DOI: 10.1134/S1064226915080021

INTRODUCTION

At optical frequencies, silver behaves as a supercritical plasma, since its complex permittivity $\varepsilon = \varepsilon' - i\varepsilon''$ satisfies the relationships $\varepsilon' < 0$, $\varepsilon'' \ll |\varepsilon'|$ [1]. The value of $\varepsilon'(\lambda)$ monotonically decreases from -1 at the wavelength $\lambda = 340$ nm to -30 at $\lambda = 800$ nm. Such a behavior of the permittivity leads to resonance phenomena occurring during scattering of electromagnetic waves by particles with a size much smaller than wavelength λ [2]. In particular, in the 3D problem of diffraction of a plane wave by a dielectric sphere, the dipole plasmon resonance occurs at $\varepsilon' = -2$, in the 2D problem of diffraction by a circular cylinder, at $\varepsilon' = -1$. Corresponding resonance frequencies for silver, $\lambda = 354$ nm and $\lambda = 340$ nm, lie in the ultraviolet part of the spectrum.

As is known, the positions of plasmon resonances in a spherical dielectric layer (nanoshell) can change in a wide range under variation in the ratio between the inner and outer shell radii [2]. In the case of a cylindrical dielectric shell, the plasmon resonance frequencies also obey this regularity [3].

Here, we investigate a nanostructure consisting of a quartz nanofiber coated with a silver layer. The aim of this study is to find the conditions for the plasmon resonances in the visible part of the optical range (400–700 nm) and study both the dipole and multipole resonances.

1. FORMULATION OF THE PROBLEM

We consider a 2D problem of diffraction of a linearly polarized plane wave

$$E_y^0 = \exp(-ikx), \quad H_z^0 = \exp(-ikx), \quad k = 2\pi/\lambda, \quad (1)$$

by a quartz wire coated with a silver layer (Fig. 1). We use the Gaussian system of units and choose the time dependence in the form $\exp(i\omega t)$, where $\omega = kc$, and c is the speed of light in vacuum.

The dependence of the permittivity on the radius of the investigated three-layered structure has the form

$$\varepsilon(r) = \begin{cases} \varepsilon_q, & 0 < r < a, \\ \varepsilon, & a < r < b, \\ 1, & r > b, \end{cases} \quad (2)$$

where ε_q and ε are the quartz and silver permittivities, respectively.

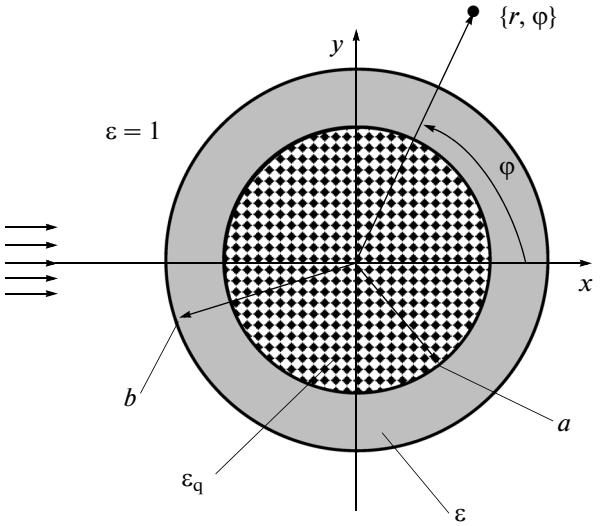

Fig. 1. Geometry of the problem.

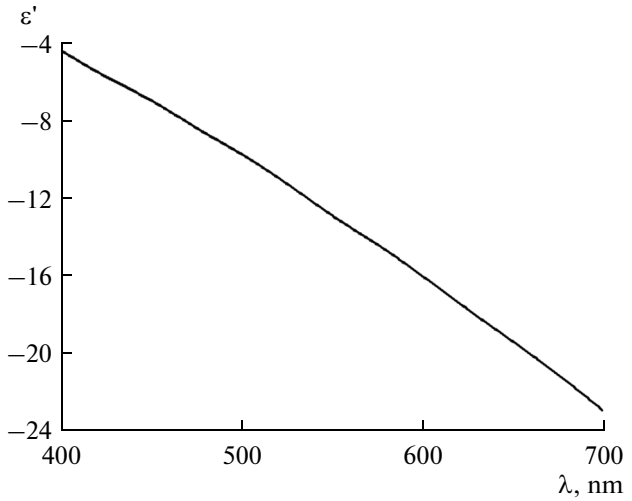

Fig. 2. Dependence of the real part of permittivity of silver ε' on the wavelength.

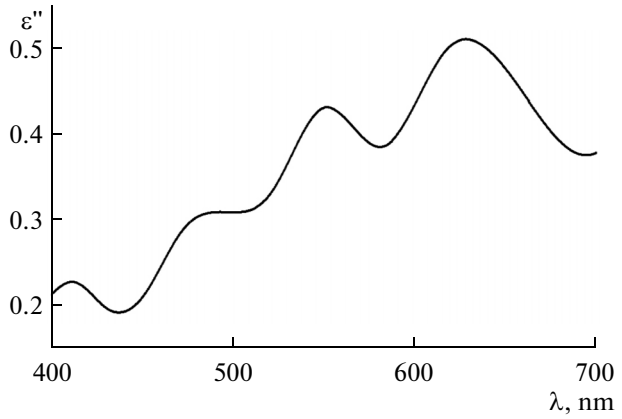

Fig. 3. Dependence of the imaginary part of permittivity of silver ε" on the wavelength.

The real and imaginary parts of the permittivity of silver in the visible spectral range of electromagnetic waves will be approximated by the functions obtained by means of cubic spline interpolation of the experimental data from [1] (Figs. 2 and 3).

Unlike silver, quartz exhibits significantly lower heat loss in the investigated frequency range and its permittivity weakly depends on λ. Therefore, we assume that the permittivity of quartz is a real quantity, $\varepsilon_q = 2.16$.

It is convenient to investigate the formulated diffraction problem with the use of component $z$of the magnetic field $U(r,\varphi) = H_z(r,\varphi)$. The boundary-value problem for function $U(r,\varphi)$ is scalar.

Total field $U(r,\varphi)$ satisfies the Helmholtz equation

$$\frac{\partial^2 U(r,\varphi)}{\partial r^2} + \frac{1}{r}\frac{\partial U(r,\varphi)}{\partial r} + \frac{1}{r^2}\frac{\partial^2 U(r,\varphi)}{\partial \varphi^2} + k^2\varepsilon(r)U(r,\varphi) = 0. \quad (3)$$

Boundary conditions for function $U(r,\varphi)$ are

$$\begin{aligned} U(a-0,\varphi) &= U(a+0,\varphi),\\ \frac{1}{\varepsilon_q}\frac{\partial U}{\partial r}(a-0,\varphi) &= \frac{1}{\varepsilon}\frac{\partial U}{\partial r}(a+0,\varphi),\\ U(b-0,\varphi) &= U(b+0,\varphi),\\ \frac{1}{\varepsilon}\frac{\partial U}{\partial r}(b-0,\varphi) &= \frac{\partial U}{\partial r}(b+0,\varphi). \end{aligned} \quad (4)$$

The incident field is specified by the function

$$U^0 = \exp(-ikr\cos\varphi). \quad (5)$$

The total field in the region $r > b$ consists of incident field U^0 and scattered field U^S

$$U = U^0 + U^S, \quad r > b. \quad (6)$$

The scattered field in the far zone must satisfy the radiation condition

$$U^S \sim \Phi(\varphi)\sqrt{\frac{2}{\pi kr}}\exp\left(-ikr + i\frac{\pi}{4}\right), \quad kr \to \infty, \quad (7)$$

where $\Phi(\varphi)$ is the scattering pattern. Components of the electric field can be expressed through function $U(r,\varphi)$:

$$E_r = \frac{1}{ik\varepsilon(r)r}\frac{\partial U}{\partial \varphi}, \quad E_\varphi = -\frac{1}{ik\varepsilon(r)}\frac{\partial U}{\partial r}. \quad (8)$$

2. QUASI-STATIC DESCRIPTION OF PLASMON RESONANCES

If the dimensions of a scatterer are small relative to the wavelength ($kb \ll 1$), then the wave field $U(r,\varphi)$ in the region $kr \ll 1$ approximately satisfies the Laplace equation

$$\frac{\partial^2 U}{\partial r^2} + \frac{1}{r}\frac{\partial U}{\partial r} + \frac{1}{r^2}\frac{\partial^2 U}{\partial \varphi^2} = 0. \quad (9)$$

Quantities ε and ε_q do not enter this equation, but they enter boundary conditions (4).

At certain discrete values of permittivity ε, homogeneous boundary-value problem (9), (4) has solutions rapidly decreasing at $r \to \infty$ [4]. These eigen oscillations can be obtained using the method of separation of variables:

$$U_m(r,\varphi) = R_m(r)\cos(m\varphi), \quad m \geq 1. \quad (10)$$

As follows from (9) and (10),

$$R_m(r) = \begin{cases} A_m r^m, & 0 < r < a, \\ B_m r^m + C_m r^{-m}, & a < r < b, \\ D_m r^{-m}, & r > b. \end{cases} \quad (11)$$

Using boundary conditions (4), we can obtain a system of homogeneous algebraic equations for unknown coefficients A_m, B_m, C_m, and D_m. Equating the determinant of the system to zero, we arrive at the dispersion equation for ε,

$$(\varepsilon + 1)(\varepsilon + \varepsilon_q) - (\varepsilon - 1)(\varepsilon - \varepsilon_q)\alpha^{2m} = 0, \quad (12)$$

where

$$\alpha = \frac{a}{b} < 1. \quad (13)$$

In [3], dispersion equation (12) was derived from the rigorous solution of problem (3)–(7) obtained using the method of separation of variables. The authors of [3] investigated resonance denominators in the Fourier expansion of the field with the use of asymptotic representations for cylindrical functions of small argument.

We denote the solutions of quadratic equation (12) by $\varepsilon_m^{\pm}$:

$$\varepsilon_m^{\pm} = -\frac{(1+\alpha^{2m})(1+\varepsilon_q) \pm \sqrt{(1+\alpha^{2m})^2(1+\varepsilon_q)^2 - 4(1-\alpha^{2m})^2\varepsilon_q}}{2(1-\alpha^{2m})}. \quad (14)$$

Both roots are negative; $-\infty < \varepsilon_m^+ < -\varepsilon_q$, $-1 < \varepsilon_m^- < 0$ and $\varepsilon_m^+\varepsilon_m^- = \varepsilon_q$.

At $\varepsilon_q = 1$, expression (14) transforms to the formulas obtained in study [4] for a cylindrical shell. In this paper, the behavior of eigenfunctions $R_m^{\pm}(r)$, corresponding to the two branches of eigenvalues, ε_m^+ and ε_m^-, was investigated. A feature of functions $R_m^+(r)$ is that they tend to zero at a certain point inside the range (a, b).

The existence of nontrivial solutions of homogeneous Laplace equation (9) means that, at small values of parameter kb, the solution of the inhomogeneous boundary problem for Helmholtz equation (3)–(7) will rapidly increase as permittivity ε approaches its eigenvalues $\varepsilon_m^{\pm}$. In this case, the only harmonic, $\cos(m\varphi)$, will dominate in the Fourier expansion.

Eigenvalues ε_m^+ significantly depend on parameter α and can vary in a wide range. In particular, at $\alpha = 0.85$, we have $\varepsilon_1^+ = -19.5$. In this case, as follows from Fig. 2, the dipole plasmon resonance ($m = 1$) arises in the long-wavelength part of the visible range.

A very important characteristic of the structure is the total scattering cross-section

$$\sigma = \frac{2}{\pi k}\int_0^{2\pi} |\Phi(\varphi)|^2 \, d\varphi. \quad (15)$$

Having calculated the dipole polarizability of the structure from the static problem, we obtain the expression for the total scattering cross section, which is valid at $kb \to 0$:

$$\sigma = \frac{\pi^2}{2} b(kb)^3 \left| \frac{(\varepsilon - 1)(\varepsilon + \varepsilon_q) - (\varepsilon + 1)(\varepsilon - \varepsilon_q)\alpha^2}{(\varepsilon + 1)(\varepsilon + \varepsilon_q) - (\varepsilon - 1)(\varepsilon - \varepsilon_q)\alpha^2} \right|^2. \quad (16)$$

At the negative value of ε, which equals

$$\varepsilon_0 = -\frac{(1+\alpha^2)(\varepsilon_q - 1) + \sqrt{(1+\alpha^2)^2(\varepsilon_q - 1)^2 + 4(1-\alpha^2)^2\varepsilon_q}}{2(1-\alpha^2)}, \quad (17)$$

scattering cross-section (16) vanishes. Certainly, rigorous expression (15) cannot vanish. However, below, we demonstrate that formula (17) makes it possible to determine wavelength λ at which function $\sigma(\lambda)$ reaches a minimum.

3. NUMERICAL RESULTS

All numerical calculations of wave fields were performed using the modified method of discrete sources [5–7] applied earlier by the authors for studying the problems of diffraction by plasma objects [8–10].

Let us consider the scattering properties of a nanostructure with parameters $b = 40$ nm and $\alpha = 0.75$. Figure 4 shows the dependence of the total scattering cross section on wavelength λ. It can be seen that, in the investigated range of wavelengths, there are two plasmon resonances ($m = 1, 2$). The permittivity eigenvalues determined from formula (14) are $\varepsilon_1^+ = -11.1$; $\varepsilon_2^+ = -5.7$. Using the plot from Fig. 2, we can determine corresponding resonance wavelengths. The obtained values are consistent with the positions of the resonance peaks in Fig. 4. Formula (17), which

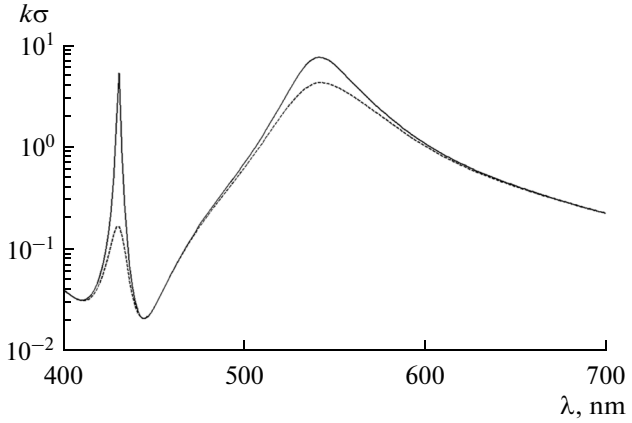

Fig. 4. Dependence of the total scattering cross-section of a structure with parameters $b = 40$ nm and $\alpha = 0.75$ on the wavelength. Solid and dashed curves correspond to $\varepsilon = \varepsilon'$ and $\varepsilon = \varepsilon' - i\varepsilon''$.

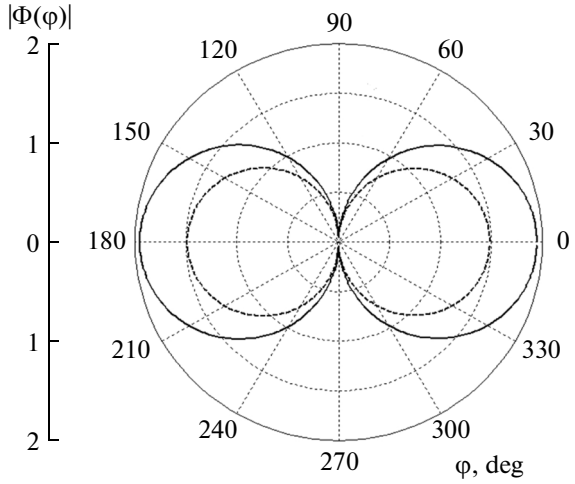

Fig. 5. Absolute values of scattering patterns of a structure with parameters $b = 40$ nm and $\alpha = 0.75$ at the wavelength of the dipole resonance ($\lambda \approx 540$ nm). Solid and dashed curves correspond to $\varepsilon = \varepsilon'$ and $\varepsilon = \varepsilon' - i\varepsilon''$.

determines zeros of the quasi-static scattering cross-section, yields $\varepsilon_0 = -4.6$. In accordance with Fig. 2, this value corresponds to the wavelength $\lambda \approx 400$ nm. It can be seen in Fig. 4 that, indeed, function $k\sigma(\lambda)$ has a minimum near $\lambda = 400$ nm.

Let us show that, far from resonance frequencies, calculations of the total scattering cross-section from approximate quasi-static formula (16) and rigorous numerical methods yield similar results. Indeed, according to Fig. 2, at $\lambda = 700$ nm, we have $\varepsilon \approx -23$; using formula (16), we obtain $k\sigma \approx 0.2$. This value is consistent with the numerically calculated data presented in Fig. 4.

Figures 5 and 6 show the absolute values of scattering patterns $\Phi(\varphi)$ at frequencies corresponding to the dipole ($m = 1$) and quadrupole ($m = 2$) resonances. Dashed lines depict the results calculated with consideration for the real loss in silver (Fig. 3). Solid curves correspond to the idealized lossless case ($\varepsilon'' = 0$). Comparison of the solid and dashed curves shows that the loss naturally reduces the level of the scattered radiation and this effect is more pronounced for the quadrupole resonance. Scattering patterns $\Phi(\varphi)$ for both the dipole and quadrupole resonances can be approximated with a high accuracy by the only harmonic, $\cos(m\varphi)$.

The spatial structure of the near field of the quadrupole oscillation is illustrated in Fig. 7, where level lines of function $|U|$ are shown. The resonance oscillation is a standing surface wave whose field is localized near the boundaries of the silver layer. Note that the quadrupole resonance cannot arise in a solid silver cylinder because of the heat loss [10].

Let us discuss evolution of plasmon resonances with an increase in the value of parameter α. The dependence of total scattering cross-section on λ for lossy and lossless structures with parameters $b = 40$ nm and $\alpha = 0.85$ is presented in Fig. 8. In contrast to Fig. 4, we have here three plasmon resonances ($m = 1$, 2, 3); the multipole resonance with index $m = 3$ exists only at $\varepsilon'' = 0$, and the dipole and quadrupole resonances are shifted toward the long-wavelength region of the visible range. Calculations have shown that scattering patterns at frequencies corresponding to these resonances are qualitatively the same as patterns in Figs. 5 and 6. Using formula (14), we obtain $\varepsilon_1^+ = -19.5$; $\varepsilon_2^+ = -9.84$; $\varepsilon_3^+ = -6.66$. As in the previous case, corresponding wavelengths are consistent with positions of resonance peaks of function $\sigma(\lambda)$.

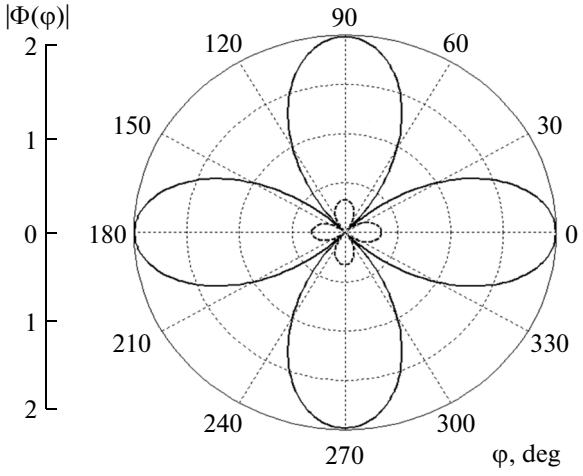

Fig. 6. Absolute values of scattering patterns of a structure with parameters $b = 40$ nm and $\alpha = 0.75$ at the wavelength of the quadrupole resonance ($\lambda \approx 430$ nm). Solid and dashed curves correspond to $\varepsilon = \varepsilon'$ and $\varepsilon = \varepsilon' - i\varepsilon''$.

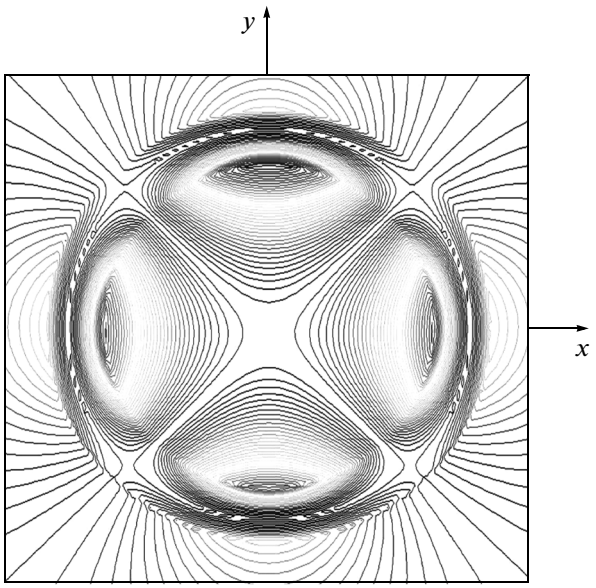

Fig. 7. Level lines of function $|U|$ of a structure with parameters $b = 40$ nm and $\alpha = 0.75$ at the wavelength of the quadrupole resonance ($\lambda \approx 430$ nm).

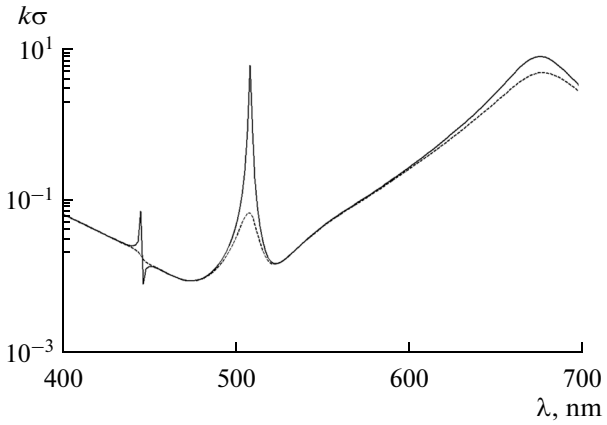

Fig. 8. Dependence of the total scattering cross-section of a structure with parameters $b = 40$ nm and $\alpha = 0.85$ on the wavelength. Solid and dashed curves correspond to $\varepsilon = \varepsilon'$ and $\varepsilon = \varepsilon' - i\varepsilon''$.

The plot of function $k\sigma(\lambda)$, shown in Fig. 8 at $\lambda \approx 475$ nm has a minimum value of 9×10^{-3}. When the silver layer is absent ($\varepsilon = 1$), the scattering cross-section of the wire is estimated in the quasi-static approximation as

$$k\sigma = \frac{\pi^2}{2}(ka)^4 \left|\frac{1-\varepsilon_q}{1+\varepsilon_q}\right|^2. \quad (18)$$

At $\lambda = 475$ nm and $a = 0.85 \times 40$ nm, this expression is equal to 2.7×10^{-2}. Thus, the deposited silver layer with a thickness of 6 nm decreases the scattering cross-section of a quartz fiber by a factor of three. This effect is independent of heat loss in silver; solid and dashed curves in Fig. 8 almost coincide near $\lambda = 475$ nm.

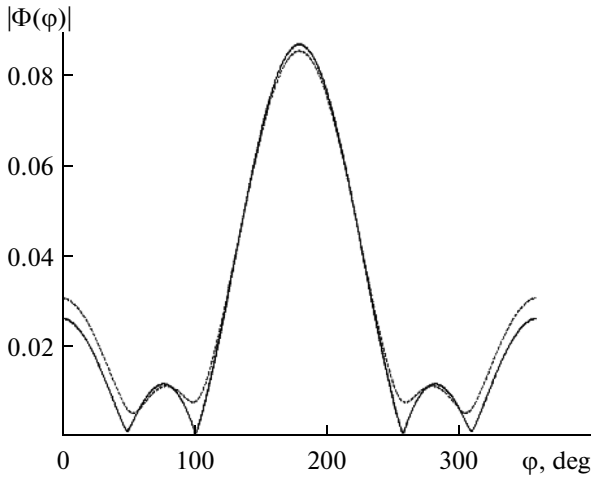

Fig. 9. Absolute values of scattering patterns of a structure with parameters $b = 40$ nm and $\alpha = 0.85$ at $\lambda = 475$ nm. Solid and dashed curves correspond to $\varepsilon = \varepsilon'$ and $\varepsilon = \varepsilon' - i\varepsilon''$.

Figure 9 shows the absolute value of scattering pattern $|\Phi(\varphi)|$ at the wavelength $\lambda = 475$ nm corresponding to the minimum of the scattered power. The dashed curve was calculated for the lossy case and the solid curve, for the lossless case ($\varepsilon'' = 0$). It appeared that this curve is described with a high accuracy by an analytical function, which is a linear combination of three harmonics, 1, $\cos\varphi$, $\cos(2\varphi)$ with real coefficients:

$$|\Phi(\varphi)| = |0.02494 - 0.03028\cos\varphi + 0.03154\cos(2\varphi)|. \quad (19)$$

Thus, at $\lambda = 475$ nm, the scattered field can be considered as a superposition of three in-phase multipole oscillations. Small value of the scattering cross-section implies that the phase of complex pattern $\Phi(\varphi)$ is close to $\pi/2$. This follows from the optical theorem [11], which, in the lossless case ($\varepsilon'' = 0$), states the following:

$$\sigma = -\frac{4}{k}\mathrm{Re}[\Phi(0)]. \quad (20)$$

In the presence of loss ($\varepsilon'' > 0$), the left-hand side of formula (20) should be supplemented with a term having the meaning of the absorption cross-section.

CONCLUSIONS

Plasmon resonances in a nanostructure consisting of a quartz fiber coated with a silver layer have been numerically investigated. The dependence of the total scattering cross-section on the wavelength has been calculated. Geometric parameters of the structure that ensure the existence of dipole and multipole plasmon resonances in the visible range of optical waves have

been determined. Scattering patterns at resonance frequencies have been calculated. It has been demonstrated that a silver layer deposited onto a quartz fiber can reduce its scattering cross-section several times.

REFERENCES

1. P. B. Johnson and R. W. Christy, Phys. Rev. B **6**, 4370 (1972).
2. V. V. Klimov, *Nanoplasmonics* (Fizmatlit, Moscow, 2009) [in Russian].
3. E. A. Velichko and A. I. Nosich, Opt. Lett. **38**, 4978 (2013).
4. A. P. Anyutin, I. P. Korshunov, and A. D. Shatrov, J. Commun. Technol. Electron. **58**, 926 (2013).
5. A. G. Kyurkchan, S. A. Minaev, and A. L. Soloveichik, J. Commun. Technol. Electron. **46**, 615 (2001).
6. A. P. Anyutin and V. I. Stasevich, J. Quant. Spectrosc. Radiat. Transf. **100** (1–3), 16 (2006).
7. A. G. Kyurkchan and N. I. Smirnova, *Mathematical Modeling in Diffraction Theory with the Use of A Priori Information on Analytic Properties of the Solution* (ID Media Pablisher, Moscow, 2014) [in Russian].
8. A. P. Anyutin and A. D. Shatrov, Pis'ma Zh. Tekh. Fiz. **39** (6), 33 (2013).
9. A. P. Anyutin, I. P. Korshunov, and A. D. Shatrov, Izv. Vyssh. Uchebn. Zaved., Radiofiz. **56**, 330 (2013).
10. A. P. Anyutin, I. P. Korshunov, and A. D. Shatrov, J. Commun. Technol. Electron. **60**, 572 (2015).
11. B. Katsenelenbaum, *High-Frequency Electrodynamics* (Wiley-VCH, Weinheim, 2006).

Translated by E. Bondareva